PHYSICAL REVIEW A **78**, 051401(R) (2008)

Three-body fragmentation of CO_2^{2+} upon *K*-shell photoionization

Z. D. Pešić,[1,2,*] D. Rolles,[1,2] R. C. Bilodeau,[1,2] I. Dimitriu,[1,2] and N. Berrah[1]
[1]*Physics Department, Western Michigan University, Kalamazoo, Michigan 49008, USA*
[2]*Advanced Light Source, Lawrence Berkeley National Laboratory, Berkeley, California 94720, USA*
(Received 17 June 2008; published 4 November 2008)

The fragmentation dynamics of CO_2 molecules subsequent to *K*-shell photoexcitation and ionization was studied using a multicoincidence ion momentum imaging technique. The detailed analysis via fragment momentum correlation plots (Newton diagrams) clearly reveals concurrent fragmentation mechanisms for the three-body dissociation of CO_2^{2+} into $C^+ + O^+ + O$, for both linear and bent geometry states of CO_2^{2+}. The experimental results are supported by a classical trajectory simulation based on a Coulomb explosion model, which elucidates energy and angular correlations between fragments for different fragmentation processes.

DOI: 10.1103/PhysRevA.78.051401 PACS number(s): 32.80.Aa, 33.15.Bh, 33.80.Eh

The energy deposited in molecules by electrons, ions, and photons leads to fragmentation into charged and neutral particles [1]. Subsequent reactions involving molecular fragments can cause chemical changes of the surrounding media. The understanding of these processes is important in diverse areas of science such as the physics and chemistry of planetary atmospheres, radiation damage of biological tissues, and surface chemistry. A complete knowledge of the fragmentation dynamics is out of reach even for very simple molecules due to the manifold of possible pathways. For example, the breaking of two or more bonds in polyatomic molecules can occur simultaneously (concerted) or sequentially, as either deferred charge separation or secondary decay [2–4]. The kinetic energy and angular distribution of the fragment ions are thus determined by the kinetic energy release (KER) in every dissociation step and by rotation and vibration of both parent molecule and intermediates [3].

Here we report a methodology to unambiguously identify different fragmentation mechanisms, applied to the $CO_2^{2+} \rightarrow C^+ + O^+ + O$ fragmentation channel, emphasizing the role of molecular bending during the fragmentation. The states with bent or linear geometry are prepared by tuning to a resonant or off-resonant photon energy [5]. The use of a multicoincidence momentum imaging technique [3,5–8] allows the direct measurement of the momentum of every detected fragment and the correlations between them, hence providing direct insight into the fragmentation mechanisms. The momentum correlation between C^+ and O^+ ions detected in coincidences is analyzed by employing fragment momentum correlation plots (Newton diagrams) [4], differentiated for selected kinetic energy ranges of the C^+ and O^+ fragments. The applied experimental technique and data analysis procedure, selecting ion pairs with certain kinetic energies, allows the identification of even weak fragmentation channels. We show that concerted fragmentation, secondary decay, and a weak deferred charge separation all occur for linear and bent molecular states.

The indication that molecules break in either a concerted or sequential manner is usually drawn from the shapes of the peaks in the covariance map [e.g., see, [2–4,9] for photoelectron-photoion-photoion coincidence (PEPIPICO) studies]. However, covariance mapping provides mostly indirect information on the fragmentation dynamics of polyatomic molecules, and the conclusions are often ambiguous and numerous peak shapes could not be fully explained [10]. For example, earlier studies of the photofragmentation [11] and electron impact fragmentation [12] concluded that a secondary decay was responsible for the fragmentation channel $C^+ + O^+ + O$, while a deferred charge separation pathway was proposed for the fragmentation in the collision with protons [13].

The experiment was performed at beamline 8.0.1 of the Advance Light Source in Berkeley, using an effusive gas target. The photon energy was tuned to the C and O $1s^{-1}2\pi_u$ resonances as well as above and below these resonances. The fragments were analyzed using a velocity-map imaging spectrometer equipped with a multihit-capable position-sensitive delay-line anode [14,15]. The radial energy scale was calibrated by imaging photoelectrons of known kinetic energy, applying reversed potentials. The mass-to-charge ratio of the ionic fragment was determined from the ion time of flight (the start signal was provided by the detection of an electron extracted opposite to the ions), which also contained information about the component of the momentum along the spectrometer axis, whereas the hit position on the position sensitive detector provided the components of the ion momentum parallel to the detector plane (p_x and p_y).

Three CO_2 photofragmentation channels leading to final states $O^+ + CO^+$, $C + O^+ + O^+$, and $C^+ + O^+ + O$ can be recognized as islands in a PEPIPICO covariance map [14,15]. The CO_2^{2+} intermediates are produced by Auger decay following the primary ionization or excitation. The electronic states of the intermediates are discussed in [16]; however, an energy-resolved electron-ion coincidence experiment is required to correlate them with the dissociation channels [17]. Figure 1 shows the KER for all three fragmentation channels for photon energies below the O *K*-edge and on resonance for the O $1s^{-1}2\pi_u$ excitation. Their branching ratios are 32%, 17%, and 51% (off resonance) and 35%, 10%, and 55% (on resonance). KER spectra and Newton diagrams below, above, and on resonance for the C $1s^{-1}2\pi_u$ excitation are similar but are not shown here. The two-body fragmentation $CO_2^{2+} \rightarrow O^+ + CO^+$ (left panels) yields fragments with kinetic

*z.pesic@fzd.de

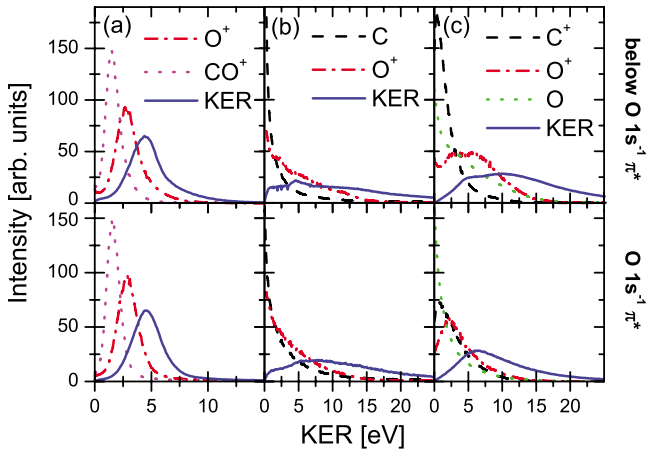

FIG. 1. (Color online) KER for different fragmentation channels of CO_2^{2+}: (a) $CO^+ + O^+$ (left), (b) $C + O^+ + O^+$ (middle), and (c) $C^+ + O^+ + O$ (right). The energy of the neutral fragments is deduced from the experimental data by applying momentum conservation. The photon energy was set to the O $1s^{-1}2\pi_u$ resonance at 535.4 (lower row) and 7.6 eV (upper row) below the resonance.

energies centered around 2.8 eV (O^+) and 1.5 eV (CO^+) and KER about 4.9 eV, with a full width at half maximum of 3.4 eV and a tail extending up to 12 eV. The three-body fragmentation $CO_2^{2+} \rightarrow C + O^+ + O^+$ (middle) is characterized by a broad KER distribution, with a slightly stronger contribution of more energetic C fragments ($E_{kin} > 5$ eV) for resonant photon energy. The strongest dependence of the KER on the photon energy is manifested for the $C^+ + O^+ + O$ channel (right). On resonance, the KER exhibits a broad peak around 7 eV, whereas for off-resonant photon energies, the KER spectrum shows a double hump, which can be decomposed into a contribution similar to that in the on-resonance case plus a higher-energy peak centered around 12 eV that extends even beyond 30 eV.

Newton diagrams for all three fragmentation pathways of the CO_2^{2+} molecular ions are shown in Fig. 2(a). A kinematically complete description of the fragmentation is possible by employing energy and momentum conservation laws that allow us to reconstruct the momentum of the neutral third particle [4,18]. We note that most coincidence momentum imaging studies to date have focused on a complete Coulomb fragmentation [5,19]. A part of these events is registered as double coincidences, due to the imperfect detection efficiency of our experimental setup (50–60 %). However, their

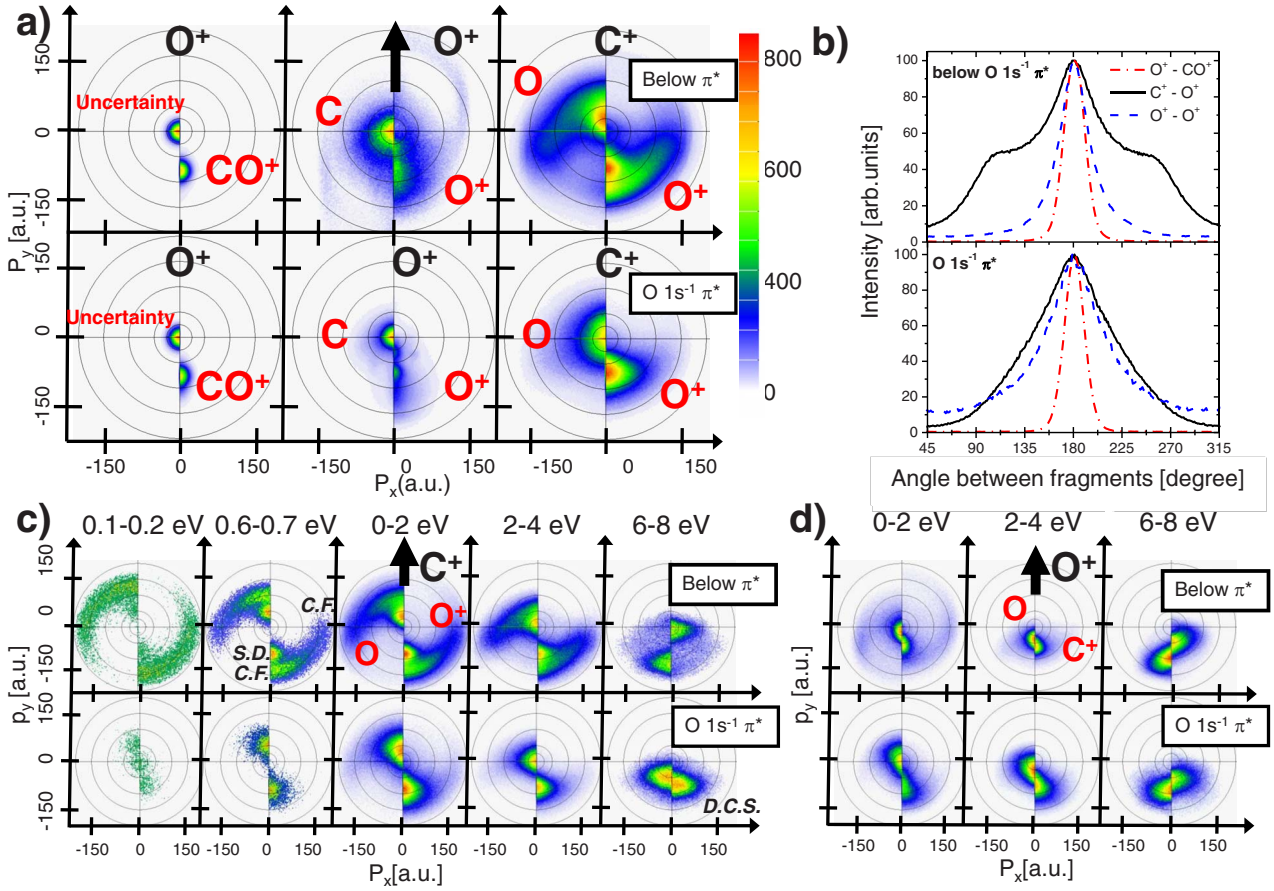

FIG. 2. (Color online) (a) Newton diagrams for CO_2^{2+} fragmenting into $\underline{O^+} + CO^+$ (left), $C + \underline{O^+} + O^+$ (middle), and $\underline{C^+} + O^+ + O$ (right) fragmentation channels. The reference ion (represented by the arrow in the middle diagram) is underlined. (b) Angle between coincident fragments detected for the above fragmentation channels. (c),(d) Newton diagrams plotted for different energy intervals (labeled above diagram) of C^+ (c) and O^+ (d) reference ions on the O $1s^{-1}\pi^*$ resonance and 7.6 eV below it.

contribution is negligible as the CO_2^{3+} production probability is only a few percent [19].

The momenta of one of the ionic fragments and of the neutral (calculated) are mapped on the right and left parts of each polar plot, with respect to the momentum of the other ion. Here, all momenta are rotated so that the reference ion points along the positive y axis. Clearly, the vector sum of the ion momenta from the two-body fragmentation into O^+ and CO^+ should equal zero, and hence gives an estimate of the uncertainty of the procedure for calculating the momentum of the neutral particle in the three-body decay. The terminal atoms from the $C+O^++O^+$ channel (two O^+ ions) also fly back to back, while the neutral C atoms remain almost at rest, with only a very small momentum perpendicular to the molecular axis. The angular spread is broader for resonant excitation. These results suggest a concerted fragmentation mechanism which is consistent with [11].

The on-resonance fragmentation into the C^++O^++O channel leads to a broad distribution of C^+-O^+ angles around 180° and small momentum of the neutral O, while a strong additional contribution, characterized by a large C^+-O^+ angular spread and larger energies of the neutral O, appears off resonance. The angular correlation is also shown in Fig. 2(b).

In order to separate different fragmentation mechanisms that are contributing to the $CO_2^{2+}\rightarrow C^++O^++O$ channel, Newton diagrams are plotted for selected kinetic energy ranges of the C^+ [Fig. 2(c)] and O^+ [Fig. 2(d)] fragments. This differentiation reveals that the distinct, circular correlation pattern for off-resonant photon energies, formed by the most energetic ($p_{xy}\approx 100$ a.u.) O^+ ions and O neutrals, exists predominantly for very low kinetic energy of the C^+ ions, while the contribution of lower-energy O^+ ions ($p_{xy}\approx 75$ a.u.), emitted back to back with respect to the C^+ ions, gains importance as the energy of the C^+ fragments increases. On resonance, only a small contribution of the circular structure is present and low-energy C^+ fragments are less abundant (see Fig. 1). The energetic neutral fragments are clearly correlated with the most energetic O^+ ions, and are emitted away from them, as can be seen from the diagrams plotted with respect to O^+ fragments [Fig. 2(d)]. At the off-resonant photon energy, a new channel seems to open above 5 eV kinetic energy of the C^+ ions, characterized by neutral O fragments with fairly substantial momentum antiparallel to C^+ and very low energy of the O^+ fragments.

In order to guide the interpretation of the experimental results, we performed classical trajectory calculations based on a Coulomb explosion (CE) model. We assumed an instantaneous rearrangement of the electrons after photoionization, which is reasonable as inner-shell vacancy relaxation times (10^{-15}–10^{-14} s) are typically a few orders of magnitude shorter than rotational and vibrational times. The fragmentation of multiply charged ions is then ruled by the Coulomb repulsion between positive, pointlike charges. The neutral fragment is taken into account allowing for fractional charges, as in [20]. In order to model a two-step fragmentation process, we allowed for a variable delay of the second bond break and a rotation of the transient ion (rigid rotor).

The results of the CE model for the C^++O^++O fragmentation channel are presented in Fig. 3, where the C^+-O^+ angle and the kinetic energy of the fragments are plotted as a function of the bond angle of the excited state, for concerted fragmentation (black circles), secondary decay (left panels), and deferred charge separation (right panels) of short- (10 fs) and long- (500 fs) lived transient CO^+ and CO^{2+} ions. Because of the known shortcomings of the CE model, particularly the oversimplification of the potential curves and the improper treatment of the neutral fragment, the calculated fragment energies cannot be expected to agree with the experimental values in terms of absolute numbers. However, the general trends and the ratios between fragment energies reflect the fragmentation dynamics adequately enough to allow direct comparisons with the experiment.

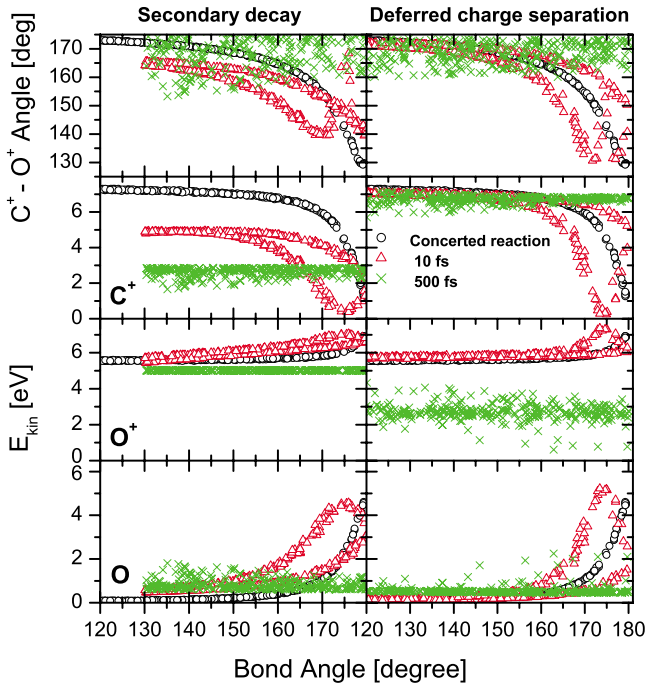

FIG. 3. (Color online) Results of the CE model for the C^++O^++O fragmentation channel for concerted, sequential, and deferred fragmentation and different lifetimes of the intermediates. The angle between C^+ and O^+ ions and the kinetic energy of C^+, O^+ and O fragments is calculated as a function of the bond angle. The scatter of the calculated points is caused by the rotational and vibrational motion.

For an instantaneous breaking of both bonds in a linear molecule (a bond angle close to 180°) the kinetic energy is shared mainly between neutral O and the O^+ ion, while the C^+ fragment ends up with a small momentum component perpendicular to the molecular axis. The fragment energy and the C^+-O^+ correlation angle strongly depends on the exact molecular geometry at the instant of the fragmentation and even zero-point vibration leads to a large angular spread. This mechanism is therefore responsible for the circular structure visible in Fig. 2 for low kinetic energies of the C^+ fragment at the off-resonance photon energy (labeled C.F.). In contrast, concerted fragmentation of a strongly bent excited state leads to back-to-back emission of very energetic C^+ and O^+ ions with a correlation angle above 170° and a neutral fragment with almost no kinetic energy. This mechanism is dominant for on-resonance photon energies, where the resonantly excited molecules have a bent geometry [5]. A

much weaker contribution from linear excited states can be seen faintly in Fig. 2(c) (0–2 eV) as well as for very energetic O^+ ions in Fig. 2(d).

In addition to concerted decay of linear and bent molecules, another decay mechanism must be evoked in order to explain the distinct "island" of less energetic O^+ fragments ($p_{xy} \simeq 75$ a.u., labeled S.D.), which is particularly well resolved below resonance for C^+ energies between 1 and 4 eV. According to our model, only a slow (>100 fs) secondary decay of CO^+ ions produces medium-energy C^+ and O^+ fragments with a correlation angle very close to 180°. This explanation is additionally supported by the nonresonant Newton diagram plotted with respect to 2–4 eV O^+ ions, which show that the energy of the neutral oxygen is similar to or slightly lower than the energy of C^+ ions. Integration over the selected regions of interest in Fig. 2 gives probabilities for the concerted fragmentation and secondary decay pathways for off-resonant ionization of 54% and 41%.

Finally, a deferred charge separation of a CO^{2+} intermediate with a rather long lifetime (>100 fs) can explain the weak but clear contribution of low-energy (<2 eV) O^+ ions. These slow O^+ ions are coincident with very low-energy neutrals and rather energetic C^+ fragments emitted opposite to the O^+ ions, as predicted by the CE model. In order to explain the momentum correlation plot for the most energetic C^+ fragments at below-resonance photon energy, which shows very slow O^+ ions and fairly energetic neutral fragments, a deferred charge separation with a lifetime close to half of a rotational period of the intermediate CO^{2+} has to be assumed. In that case, a very slow O^+ ion can be produced if the moving CO^{2+} ion rotates enough that the O^+ gains velocity antiparallel to the velocity of the intermediate CO^{2+}. Such a process would also produce faster C^+ ions. As this channel is very weak (about 5%), this assumption is not entirely unreasonable.

In conclusion, we have clearly identified three different fragmentation mechanisms in the three-body fragmentation of CO_2^{2+} after excitation by synchrotron light in the vicinity of inner-shell resonances. The analysis of the measured momenta correlation uncovers even a weak deferred charge separation in addition to the strong concerted fragmentation and secondary decay channels for both linear and bent molecular states. The prediction for the mean KER and the momentum correlation between fragments by the CE model are reasonable and support our interpretation of the experimental results. This methodology can be applied to any polyatomic molecule.

This work is supported by BES, DOE, and CSGB divisions.

[1] D. Mathur, Phys. Rep. **225**, 193 (1993).
[2] J. H. D. Eland, Chem. Phys. Lett. **203**, 353 (1993).
[3] S. Hsieh and J. Eland, J. Phys. B **30**, 4515 (1997).
[4] S. Hsieh and J. Eland, Rapid Commun. Mass Spectrom. **9**, 1261 (1995).
[5] Y. Muramatsu *et al.*, Phys. Rev. Lett. **88**, 133002 (2002).
[6] U. Becker, J. Electron Spectrosc. Relat. Phenom. **112**, 47 (2000).
[7] R. Dörner, V. Mergel, O. Jagutzki, L. Spielberger, J. Ullrich, R. Moshammer, and H. Schmidt-Böcking, Phys. Rep. **330**, 95 (2000).
[8] D. Dowek, M. Lebech, J. C. Houver, and R. R. Lucchese, J. Electron Spectrosc. Relat. Phenom. **141**, 211 (2004).
[9] J. H. D. Eland, Mol. Phys. **61**, 725 (1987).
[10] J. H. D. Eland, Laser Chem. **11**, 259 (1991).
[11] T. Masuoka, E. Nakamura, and A. Hiraya, J. Chem. Phys. **104**, 6200 (1996).
[12] C. Tian and C. R. Vidal, Phys. Rev. A **58**, 3783 (1998).
[13] P. Moretto-Capelle, D. Bordenave-Montesquieu, and A. Bordenave-Montesquieu, J. Phys. B **33**, L539 (2000).
[14] Z. D. Pešić, D. Rolles, M. Perri, R. Bilodeau, G. Ackerman, B. Rude, A. Kilcoyne, J. Bozek, and N. Berrah, J. Electron Spectrosc. Relat. Phenom. **155**, 155 (2007).
[15] D. Rolles, Z. Pešić, M. Perri, R. Bilodeau, G. Ackerman, B. Rude, A. Kilcoyne, J. Bozek, and N. Berrah, Nucl. Instrum. Methods Phys. Res. B **261**, 170 (2007).
[16] E. Kukk, J. D. Bozek, and N. Berrah, Phys. Rev. A **62**, 032708 (2000).
[17] P. Morin, M. Simon, C. Miron, N. Leclercq, E. Kukk, J. D. Bozek, and N. Berrah, Phys. Rev. A **61**, 050701(R) (2000).
[18] B. Bapat and V. Sharma, J. Phys. B **40**, 13 (2007).
[19] K. Ueda and J. Eland, J. Phys. B **38**, S839 (2005).
[20] S. Hsieh and J. Eland, J. Chem. Phys. **103**, 1006 (1995).